Chapter 1

Nordic 5-Machine (N5) Test System

1.1 Introduction

The N5 test system is developed with the intention for studying frequency containment reserves (FCR) in a low-inertia power system. The system is fictitious but has dynamical properties that are similar to the Nordic synchronous grid. The network is divided into 5 areas based on geographical location and the dominant means of synchronous power production. Loads, synchronous machines, and wind turbines are lumped up into a single large component at each bus.

The model is implemented in Simulink Simscape Electrical [1]. The simulation software readily allows for studying voltage stability, transient stability considering load disturbances, balanced or unbalanced short circuit faults, et.c. Thus, the model can also be adjusted to study phenomena beyond FCR. This however, falls outside the scope of this work. The purpose of this model is to study FCR control limitations and control design in a heterogeneous grid. The Nordic grid is chosen as it is a relatively small grid dominated by hydro power and thus provides a illustrative, and relevant test case.

1.2 Modeling Choices

The network consist of five areas. Following the numbering in Fig. 1.1:

1–3. Norway, Northern Sweden, and Northern Finland, respectively. Hydro power production centers with some local loads and wind power production.

4. Southern Sweden and Eastern Denmark. Large load center with some local production from thermal power plants and wind turbines.

5. Southern Finland, load center with some local thermal power production.

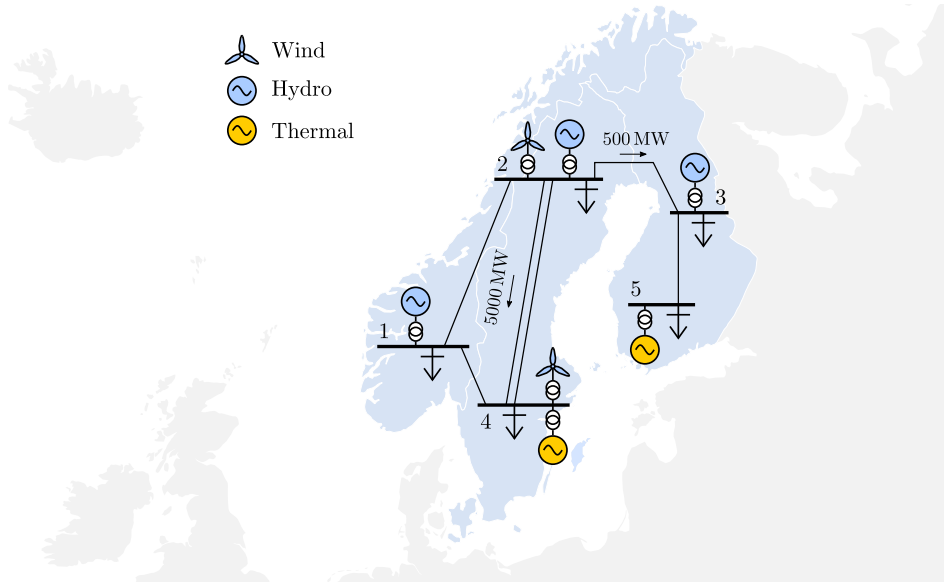

Figure 1.1: One-line diagram of the N5 test system.

The model is designed for studying FCR control in a low-inertia grid. The most significant properties are therefore: the combined kinetic energy, W_{kin}, of the synchronous machines; and the FCR control.

1.2.1 Inter-Area Modes

The Nordic-5 machine model is detailed enough to capture some of the dominant inter-area modes in the Nordic grid. The transmission line parameters are tuned so that the two dominant inter-area modes roughly matches the

- 0.33 Hz interarea mode between Finland and South Norway and Sweden; and
- 0.48 Hz interarea mode between Norway and South Sweden

observed in the Nordic grid [2].

Estimating transmission line parameters

The following procedure was used to give a "first guess" for the transmission line parameters, and to initiate the tuning process.

Using the 0.33 Hz mode as an example.

1. Let Ω_0 be the frequency of the considered mode.
2. Assume all buses to have p.u. voltage V_0.

3. Let M_1 and X_1 be the total machine inertia constant and reactance (including transient machine reactances and transformers) at buses 1 and 4.

4. Let M_2 and X_2 be the inertia and reactance at buses 3 and 5.

5. The total reactance of the transmission corridor between area 1 and 2 should then be
$$X_{\text{line}} = \left(\frac{M_1 + M_2}{\Omega_0^2 M_1 M_2} - X_1 - X_2 \right) V_0^2.$$

1.2.2 Load Modeling

The N5 test system is designed to study the dynamics of frequency controlled FCR when subject to large disturbances, i.e., large-signal analysis. The considered energy sources include hydro plants, thermal plants, wind turbines, battery storages, et.c. For the intended applications, voltage dynamics are not of interest. Therefore, we choose to model all active power loads as constant power loads. This is a discrepancy from the real system. For example, in [3] active power loads are modeled as constant current loads and reactive power loads are modeled as constant impedance loads.

Constant Power Loads

With constant power loads, voltage drops has no effect on the FCR. Thus, it is irrelevant, where in the network, disturbances occur. The dynamics relevant for FCR can therefore be accurately described by a first-order swing equation. For instance, consider the case where the power system is operated with a large power flow from bus 2 to bus 4. This means that there is a large load angle between bus 2 and 4, and a voltage drop over the north-south transmission corridor. Now consider a disturbance in the form of a generator trip, or the disconnection of a importing HVDC link in the south. This result in a negative power balance in the over-all system, consequently, frequency will decline. The disturbance will also increase the load angle between bus 2 and 4, and thereby the voltage drop over the north-south transmission corridor. Consequently, the power drawn by voltage dependent loads will decrease in the souther load centers. This effect, contributes positively to the FCR. However, it is hard to include this effect in the analysis since the FCR contribution from voltage dependent loads depends on:

- where the disturbances occur;
- if loads are constant power, constant current, constant impedance, or somewhere in between;
- how large loads are, in absolute numbers, at each bus;
- short-term and long-term voltage controllers and tap-changing transformers.

Table 1.1: Generator p.u. data [3].

Type	X_d	X_q	X'_d	X'_q	X''_d	X''_q	X_{L}	T'_{d0}	T'_{q0}	T''_{d0}	T''_{q0}	X_{trafo}	H
Hydro	1.1	0.7	0.25	-	0.2	0.2	0.15	5.0	-	0.05	0.1	0.15	3
Thermal	2.2	2.0	0.3	0.4	0.2	0.2	0.15	7.0	1.5	0.05	0.05	0.15	6

Moreover, the PSSs are less effective with constant power loads, compared to a system with voltage dependent loads. This reduces the stability of interarea modes. Thus, the pros of assuming constant power loads are the following:

1. Since bus voltages have no effect on loads, the absolute value of active and reactive loads are irrelevant for the FCR dynamics. This significantly simplifies the design of new test cases and load flows.

2. The model can be viewed as a worst-case realization with respect to FCR and stability of interarea modes.

1.3 Dynamic Models

1.3.1 Generator

The machine is modeled using the synchronous machine model available in the Simscape Electrical library [1]. Parameter values, shown in Table 1.1 are adapted from the Nordic 32 Cigré test system [3].

- Salient pole model for the hydro generators.
- Round rotor model for the thermal generators.

1.3.2 Excitation System

Exciters are modeled using the standard exciton system block available in the Simscape Electrical library [1]. The block models an IEEE type 1 synchronous machine voltage regulator combined to an exciter. The implemented model, shown in Fig. 1.2, uses the default parameter settings. Terminal voltage is controlled using feedback from voltage measurement $\hat{V}$. Neglecting fast exciter dynamics, the exciter are modeled as a constant, controlling the field voltage V_f. The main regulator also takes an auxiliary input, V_{stab}, from a PSS.

1.3.3 Power System Stabilizer (PSS)

PSSs are modeled using a typical fourth-order controller [4], shown in Fig. 1.3. The PSS is implemented with feedback from $P_m - P_e$. This is the accelerating force acting on the rotor. Another popular measurement to use, is the machine speed.

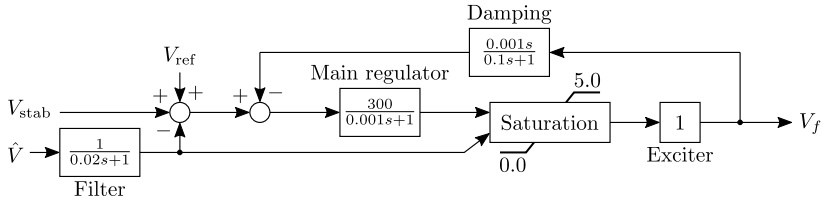

Figure 1.2: Block diagram of machine excitation system.

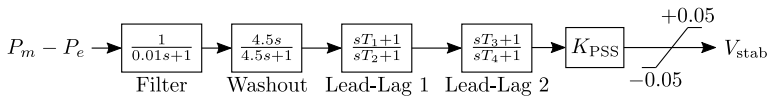

Figure 1.3: Block diagram of PSS.

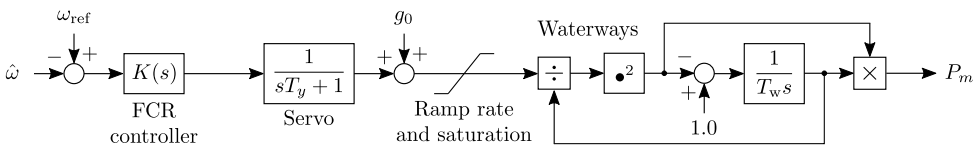

Figure 1.4: Block diagram of hydro governor.

Table 1.2: Hydro parameters adapted from [5].

Bus	T_y	T_{w}	g_0
1	0.2	0.7	0.8
2	0.2	1.4	0.8
3	0.2	1.4	0.8

The lead-lag filter time constants T_1–T_4 are tuned to achieve the correct phase compensation for each individual machine. These, along with the controller gain K_{PSS} are tuned for each specific load flow.

1.3.4 Hydro Governor

The hydro governor model implemented in this work is an adaption of the hydro governor model available in the Simulink Simscape Electrical library [1]; modified to allow a general linear FCR controller, $K(s)$, instead of the predefined PID/droop control structure as shown in Fig. 1.4. The nonlinear second-order model is useful for large-signal time-domain simulations. Servo time constant T_y and the water time constant T_{w}, shown in Table 1.2, are adapted from the case study in [5]. The initial gate opening g_0 are assumed to be 80 % for all governors.

1.3.5 Thermal Governor

Active power from thermal machines are assumed to be 90 % of rated power. Thermal machines are not participating in FCR. Therefore, dynamic governor models are not included.

1.3.6 Load

Active power loads are modeled as constant power loads, as motivated in Section 1.2. Reactive power loads and shunts are modeled as constant impedance loads. With constant load modeling, the absolute value of active power loads have no big impact on system dynamics. Loads are therefore selected according to Tables 1.5 and 1.7 to give the desired inter-area power flows. Reactive power loads are set to zero and shunt capacitors are tuned according so that bus voltages are close to nominal in the initial load flow.

Active power loads have a constant frequency dependency, K_L, distributed proportionally on all buses so that the frequency dependent load at each bus is $\Delta P_L = K_L \omega_e$. For the simulation, the local frequency, ω_e, is obtained from the local phase angle, θ, filtered through a second-order filter,

$$\omega_e = s \frac{1}{s0.01 + 1} \frac{1}{0.001s + 1} \theta$$

so that the simulation can run a reasonable speed. For the linearization, frequency dependent loads are implemented using the machine speed from the closest synchronous machine. This has no significant impact on the result, but simplifies the linearization.

1.3.7 Transmission Line

Transmission lines are modeled using the distributed parameters line model available in the Simulink Simscape Electrical library [1]. The ac frequency is 50 Hz and the line is assumed to be a continuously transposed three phase line. Using default values:

- The positive and zero sequence resistance is 0.01273 and 0.3864 Ω/km,
- The positive and zero sequence inductance is 0.9337 and 4.1264 mH/km,
- The positive and zero sequence capacitance is 12.74 and 7.751 nF/km,

respectively.

The line parameters used in the 240 and 110 GWs test cases are shown in Tables 1.3 and 1.4. The parameters where first selected using the procedure described in Section 1.2.1. For the 110 GWs, transmission lines are modified (length reduced) to ensure transient stability when simulating a large load disturbance at bus 1.

Table 1.3: 240 GWs test case.

Buses	Length [km]
1–4	250
2–4	100
2–3	100
3–5	150
1–2	400

Table 1.4: 110 GWs test case.

Buses	Length [km]
1–4	220
2–4	100
2–3	100
3–5	150
1–2	300

Table 1.5: Load flow of the 240 GWs test case.

Bus	W_{kin} [MWs]	P_m	P_L	Q_L	Q_{sh} [MW]	V [p.u.]	θ [°]
1	67 500	18 000	18 000	-	540	0.996	40.0
2	45 000	12 000	6500	-	1195	0.988	72.2
3	7500	2000	2000	-	60	0.996	66.6
4	73 333	11 320	16 000	-	2480	0.994	22.0
5	46 667	7000	7500	-	725	1.004	58.4

1.4 Load Flows

Generators are connected to network buses through a transformer. In the load-flow, machines are initiated as PV-buses, with machine terminal set to 1 p.u. Machine 4 is set as slack bus so that its terminal voltage is $1\angle 0°$.

The active power balance at the 5 network buses are selected so that there is a 5000 MW north-south power flow from bus 2 to bus 4, and a 500 MW west-east power flow from bus 2 to bus 5. As motivated in Section 1.2, only the active power balances are relevant. Shunt elements are tuned to achieve satisfactory bus voltages, without having to implement load transformers with different tap-ratios. With loads connected directly to each bus, the N5 test system have a total of 10 network buses.

1.4.1 240 GWs Test Case

The parameter setting and load flow result for the 240 GWs test case are shown in Table 1.5. Machine ratings and active power set-points are adapted from [5].

The PSS parameter setting for the 240 GWs test case are shown in Table 1.6. The table also list the modal frequency and damping ratios with (and without) PSS. The PSS tuning procedure is described in Section 1.5.

1.4.2 110 GWs Test Case

The parameter setting and load flow result for the 110 GWs test case are shown in Table 1.5.

The PSS parameter setting for the 110 GWs test case are shown in Table 1.8. The table also list the modal frequency and damping ratios with (and without) PSS.

Table 1.6: PSS settings and interarea modes for the 240 GWs test case. Values in parenthesis indicate modal parameters with PSS.

Bus	T_1	T_2	T_3	T_4	K_{PSS}	freq. [Hz]	damping [%]
1	0.1323	0.6743	0.1323	0.6743	0.15	-	-
2	0.1077	0.4456	0.1077	0.4456	0.6	0.73 (0.72)	-1.9 (7.2)
3	0.0527	0.3223	0	0	0.15	1.22 (1.23)	-1.2 (8.7)
4	0.1315	0.6785	0.1315	0.6785	0.15	0.53 (0.53)	1.4 (4.8)
5	0.1829	0.9771	0.1829	0.9771	0.15	0.38 (0.37)	0.3 (3.9)

Table 1.7: Load flow of the 110 GWs test case.

Bus	W_{kin} [MWs]	P_m	P_L	Q_L	Q_{sh} [MW]	V [p.u.]	θ [°]
1	33 750	9000	9000	-	270	0.993	41.6
2	22 500	6000	500	-	1015	0.982	70.7
3	7500	2000	2000	-	60	0.998	65.1
4	33 333	5253	10 000	-	2300	0.994	21.8
5	13 333	2000	2500	-	575	1.02	57.2

Table 1.8: PSS settings and interarea modes for the 110 GWs test case. Values in parenthesis indicate modal parameters with PSS.

Bus	T_1	T_2	T_3	T_4	K_{PSS}	freq. [Hz]	damping [%]
1	0.1042	0.4392	0.1042	0.4392	0.15	-	-
2	0.0519	0.5546	0	0	0.6	0.94 (0.94)	-6.7 (4.4)
3	0.0540	0.3156	0	0	0.15	1.22 (1.23)	-1.4 (11.7)
4	0.1071	0.4274	0.1071	0.4274	0.15	0.74 (0.74)	2.3 (8.2)
5	0.1290	0.5423	0.1290	0.5423	0.15	0.60 (0.59)	-1.2 (4.4)

Note that the two major interarea modes have a higher freqeucny for the 110 GWs test case, as compared to the 240 GWs case. This is due to the lower ratings of the connected machines, and due to the adjusted transmission line parameters in Table 1.4.

1.5 PSS Tuning Procedure

PSSs are tuned to obtain a stable working example, with interarea mode shapes and damping ratios similar to the real system properties identified in [2, 5].

1. Linearize the system and identify poorly damped interarea modes. The four interarea modes for the 240 GWs test case are shown in Fig. 1.5.

2. Calculate the residues [4] of the 5 machines for each mode. Residues associated with the 240 GWs test case are shown in Fig. 1.6.

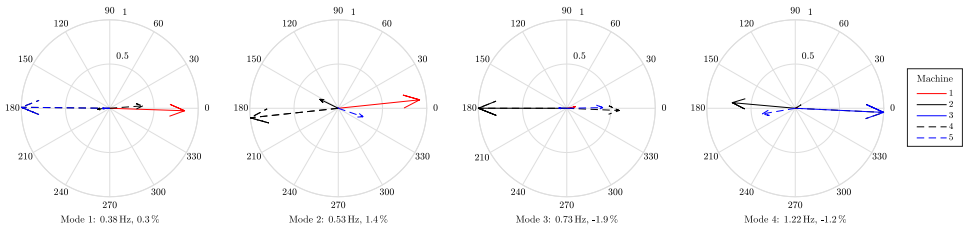

Figure 1.5: Compass plot of the undamped interarea modes in the 240 GWs test case.

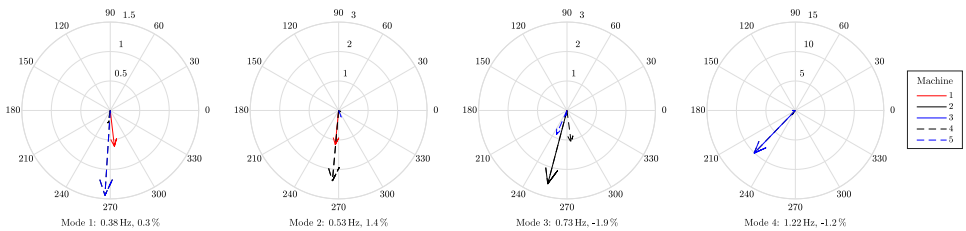

Figure 1.6: Residues, with measurement of $P_m - P_a$, in the 240 GWs test case.

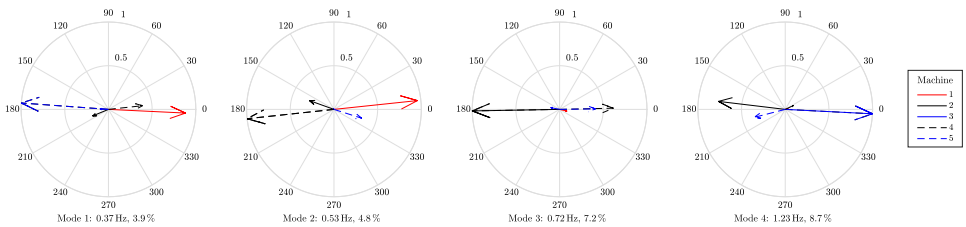

Figure 1.7: Compass plot of the interarea modes (with PSS) in the 240 GWs test case.

3. Starting with the most poorly damped mode: Select the machine with the highest participation factor (some manual adjustments may be required) and tune the time constants T_1–T_4 so that the residue, with phase compensation, becomes 180°.

4. For the following modes, in ascending order according to damping ratio, follow the same procedure. Exclude machines that have already been tuned.

5. A system of 5 machines will have 4 modes. The remaining machine is tuned for the mode in which it has the highest participation factor.

6. Controller gains are tuned manually to achieve around 4 % damping of the low-frequency modes [2] and around 8 % for the faster modes. The four interarea modes (with PSS) for the 240 GWs test case are shown in Fig. 1.7.

Bibliography

[1] Hydro-Québec and The MathWorks, "Simscape Electrical Reference (Specialized Power Systems)," Natick, MA, Tech. Rep., 2020.

[2] K. Uhlen, L. Vanfretti, M. M. de Oliveira, A. B. Leirbukt, V. H. Aarstrand, and J. O. Gjerde, "Wide-area power oscillation damper implementation and testing in the Norwegian transmission network," in *Proc. IEEE/PES General Meeting*, San Diego, CA, Jul. 2012, pp. 1–7.

[3] CIGRÉ, "Long term dynamics phase II final report," Tech. Rep. Task Force 38.08.08, Mar. 1995.

[4] P. Kundur, *Power System Stability and Control*. New York: McGraw-Hill, 1994.

[5] L. Saarinen, P. Norrlund, U. Lundin, E. Agneholm, and A. Westberg, "Full-scale test and modelling of the frequency control dynamics of the Nordic power system," in *IEEE Power and Energy Society General Meeting*, Boston, MA, Jul. 2016, pp. 1–5.

[6] J. Björk, D. V. Pombo, and K. H. Johansson, "Variable-speed wind turbine control designed for coordinated fast frequency reserves," p. 8, unpublished.

[7] K. Uhlen, L. Warland, J. O. Gjerde, O. Breidablik, M. Uusitalo, A. B. Leirbukt, and P. Korba, "Monitoring amplitude, frequency and damping of power system oscillations with PMU measurements," in *IEEE Power and Energy Society General Meeting - Conversion and Delivery of Electrical Energy in the 21st Century*, Pittsburgh, PA, Jul. 2008, pp. 1–7.